

# An Experimental Study on the Topography Effects on the Seismic Response of Combined Piled Raft Foundation

Hassan Panahpour<sup>1</sup>, Tohid Akhlaghi<sup>1\*</sup>, Masoud Hajjalilue-Bonab<sup>1</sup>

<sup>1</sup> Department of Soil and Foundation Engineering, Faculty of Civil Engineering, University of Tabriz, 29 Bahman Boulevard, 5166616471 Tabriz, East Azerbaijan Province, Iran

\* Corresponding author, e-mail: [takhlaghi@tabrizu.ac.ir](mailto:takhlaghi@tabrizu.ac.ir)

Received: 25 April 2023, Accepted: 01 December 2024, Published online: 17 January 2025

## Abstract

The effect of topography on the amplification of seismic forces has been considered in regulations, and they have deemed the use of the seismic force amplification coefficient in the design of adjacent earth-retaining structures necessary. However, the impact of settlement-reducing or anti-sliding piles under the building foundation on the applied acceleration to the foundation is generally not addressed in regulations, and it is necessary to carefully examine this issue for the optimal design. This study sought to empirically assess the impact of using piles as Combined Piled Raft Foundation (CPRF) positioned on the top of slopes, with different slope angles, on the seismic behavior of slopes, scaled at 1/25<sup>th</sup>, through shaking table experiments. Six sinusoidal waves were created as input motions to simulate a range of earthquake scenarios, applied to the models to collect data for analyzing the seismic response of the system. No.161 Firouzkooch sand was utilized as the soil in this investigation. The amplification factor (AF) of various locations was used to examine the seismic response of the system. The findings underscore the importance of the amplification factor as a critical parameter in evaluating the seismic response of foundations situated on slope crests. Additionally, Implementing CPRF and longer piles had a mitigating effect on accelerations at most points and improved the seismic response of the slopes, reducing amplification factor and led to less damages. Furthermore, the slope angle was shown to significantly influence the seismic response, with steeper angles generally resulting in higher amplifications at the slope crest.

## Keywords

seismic response, slope, pile, CPRF, amplification, shaking-table test

## 1 Introduction

Currently, urban development has led to the expansion of construction into suburban areas. In some regions, construction sites are located on irregular terrain, influencing the seismic response of the ground significantly as observed in earthquake data [1–4]. Particularly, structures situated on hillslopes and ridges have been shown to sustain more damage compared to those built on flat ground areas [5–7]. An essential parameter to analyze the seismic response of systems is the amplification factor (AF), which indicates the ratio of Peak Ground Acceleration (PGA) at a specific point to the input motion from the source of excitation. The phenomenon of topographic amplification of earthquake ground motion has been extensively documented in scientific literature [3, 8, 9]. The interaction of soil properties, structural dynamics, and site topography can lead to intense ground motion and damage in certain locations [10]. Experimental studies on shaking

tables have demonstrated that slope elevation and stratigraphy significantly influence the seismic response of slopes, with failure predominantly occurring near the surface of the slope [9–14]. Additionally, it has been noted that at a distance of 2–3 times the slope height ( $H$ ) from the crest, the acceleration is amplified due to topographic irregularities. Furthermore, structures near the slope crest experience the greatest impact of seismic response due to topographic conditions [8]. Limited research has investigated the effect of slope angle on the seismic response of slopes, with fewer studies focusing on reinforced slopes. Findings indicate that an increase in slope angle leads to heightened acceleration near the slope crest [15–17]. Moreover, Zhang et al. [18] highlighted the significant role of slope geometry in seismic wave propagation on the surface. Qi et al. [13] conducted a study using numerical 3D models of slopes subjected to multidirectional seismic loads, evaluating the

impact of variables such as soil type, slope height, angle, and peak acceleration on the amplification factor of ground motions. Results showed the influence of topographic amplification relative to the dynamic properties of systems, with an increase in slope height or angle not necessarily correlating with a proportional increase in amplification.

Moreover, the maximum topographic amplification factor predominantly occurs near the slope crest within a distance from the slope crest to the height of the slope ( $x/H = 1.5$ ). Many factors are intensifying seismic ground motions near the slopes, some of which can be categorized as follows: topography, stratigraphy, soil inhomogeneity, and nonlinear behavior of materials [19]. Previous studies imply that the reflection of the waves colliding with the slope is the main factor in creating the amplification of motions adjacent to slope topography [18]. Also, based on Fig. 1 waves generated within the slope due to seismic motions include input vertical SV waves, waves reflected from the slope surface and soil layers, Rayleigh waves, and *P* waves. According to the reported studies and field measurements, the amplification value was in the range of 2–5 times [20, 21], and some other studies, more than

10 times the free field [22, 23]. However, in most numerical analyses, the amplification factor near the slope crest was in the range of 1–3 [8, 13, 14, 18, 24, 25].

Also, different building codes consider the effect of increased shear force imposed on structures located on slopes or in close proximity to them through the topographic amplification factor (ST). For example, this factor is according to "Iranian Code of Practice for Seismic Resistance Design of Buildings" (Standard No. 2800) [26] as shown in Table 1.

Using piles has been one of the common ways to enhance the dynamic performance of a foundation built in sloping areas [27]. In some cases, piles are used in the slope body as anti-slide piles and sometimes connected to foundations on the slope crest as piled foundations. Many researchers have evaluated the effect of the anti-slide pile on amplification and seismic response experimentally and numerically. Studies on anti-slide piles resulted in the reduction of amplification and slope body deformation [28–34]. Besides, there have been a rare number of studies to investigate the effect of the soil-structure interaction (SSI) concerning slope topography. Some studies

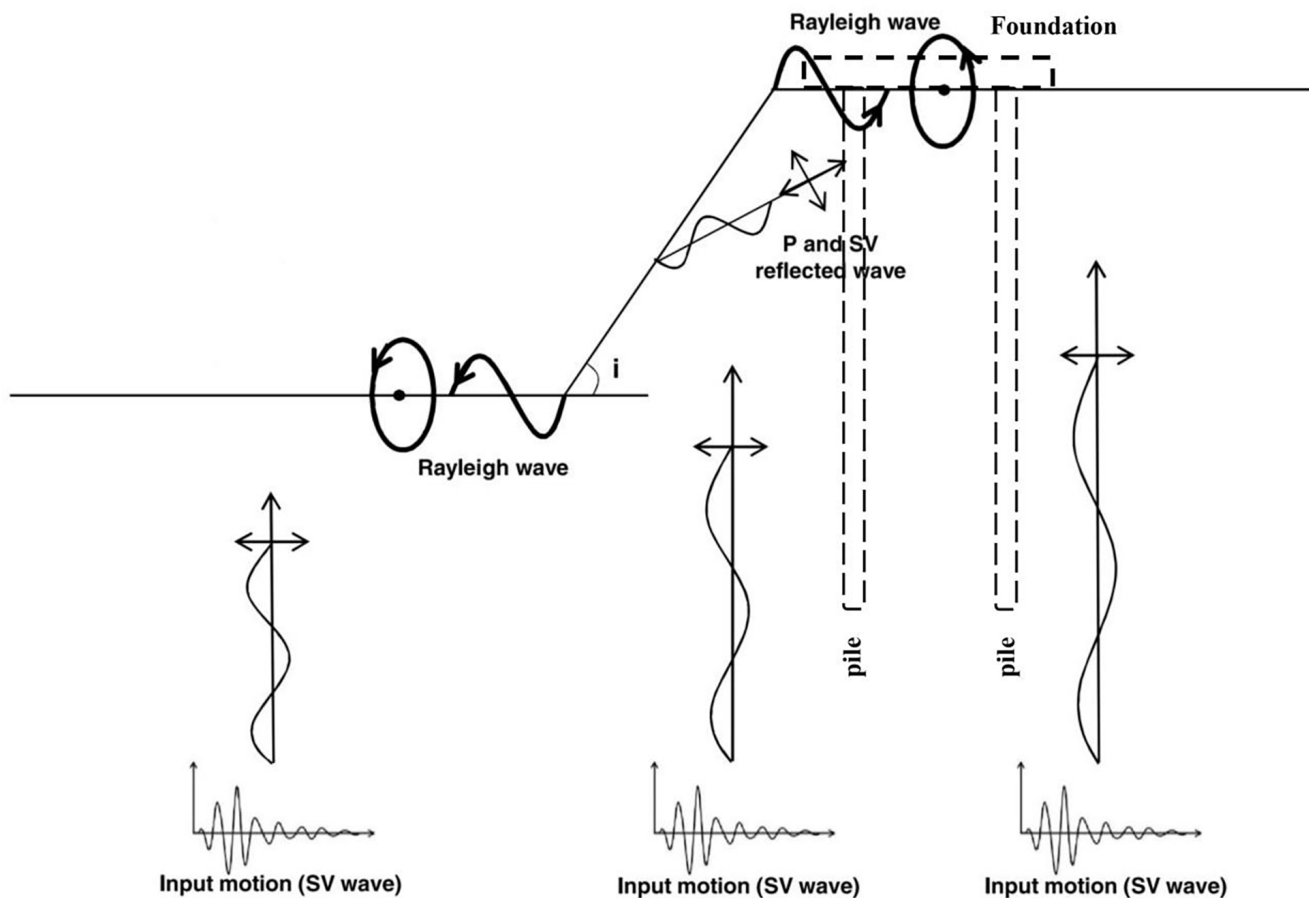
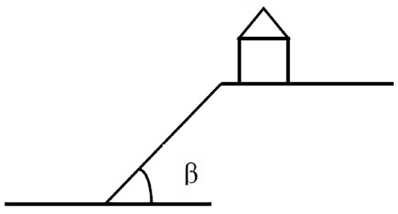
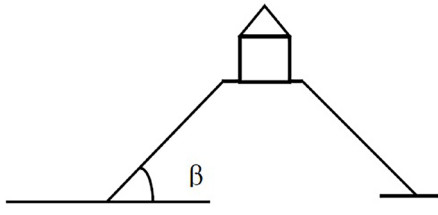



Fig. 1 Schematic illustration of incoming and induced waves in the soil medium due to the presence of CPRF on the slope crest

**Table 1** Topographic amplification factor – "Iranian Code of Practice for Seismic Resistance Design of Buildings" (Standard No. 2800) [26]

Slope	$\beta$ (deg.)	ST
	$>15$	$\geq 1.2$
	15 to 30	$\geq 1.2$
	$>30$	$\geq 1.4$

were carried out using single and group piles in slope employing numerical and experimental methods [35, 36]. However, on the slope crest, the amplification led to stronger motions and it is important to consider the topography-soil-structure interaction (TSSI) in the analyses of the seismic response of foundations constructed in the topographic areas. In this regard, some studies have been conducted based on piled foundations. A type of foundation is known as the Combined Piled Raft Foundation (CPRF).

When piles are used, amplification factor may decrease for the following reasons:

- **Reduced Stiffness:** Piles designed for controlled sliding have lower stiffness compared to rigidly embedded piles. This reduced stiffness allows them to deform more easily during ground shaking, absorbing energy in the process.
- **Frictional and passive Resistance:** The sliding interface between the pile and the surrounding soil generates frictional and passive resistance as the structure moves. This frictional force helps dissipate seismic energy by converting it into heat.
- **Soil Plasticity:** The soil itself can exhibit plastic behavior during seismic shaking, leading to energy dissipation at the pile-soil interface. Plastic deformation in the soil absorbs energy and reduces the seismic forces transmitted to the pile.
- **Dynamic Soil-Structure Interaction (SSI):** The interaction between the pile and the surrounding soil during seismic events can lead to energy dissipation. Dynamic SSI effects can influence the distribution of seismic forces and contribute to energy dissipation through soil-pile interaction.

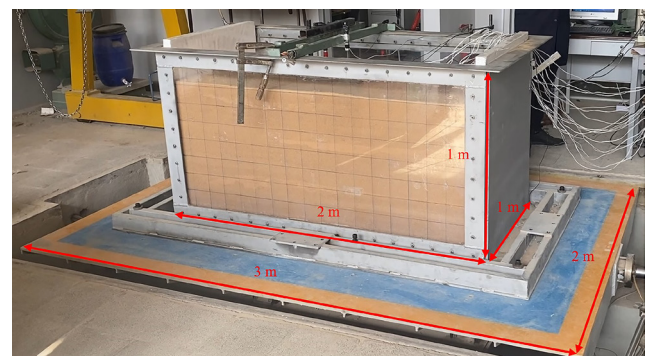
Considering the points mentioned, it is appropriate to conduct a separate investigation to examine the precise effect of piles on reducing the amplification factor on foundations based on sloping ground, and as far as we know, such research has not been conducted before. To fill the previous studies' gap, this experimental study, using a series of shaking table tests, was programmed and performed to better understand the seismic response of the slope with a CPRF and compare the different characteristics between a flat and sloping grounds with various angles (constant height). The effects of acceleration and frequency of input motions, slope angle and pile length on the dynamic response of the system were considered in the tests.

To achieve this goal, models were initially constructed without piles, and then, after adding piles to the model, the effect of using piles in reducing the amplification effects of acceleration and seismic forces was investigated under various dynamic excitations. Subsequently, by constructing physical models with different slope angles, the amplification factor of acceleration in different topographies was examined and compared. In the conclusion section, amplification factors corresponding to each slope were considered.

## 2 Testing apparatus and procedure

### 2.1 Shaking table apparatus

A uniaxial shaking table located in the geotechnical laboratory of the University of Tabriz was used in this study (as shown in Fig. 2). The dimension of the shaking table deck is 200 cm  $\times$  300 cm (width  $\times$  length). Input motions could be applied as time history and sinusoidal excitations up to 6 tons of the maximum payload mass with a wide range of frequencies between 0.1 and 50 Hz, available to apply at the base of the deck by hydraulic servo actuator. A rigid rectangular box with dimensions of 200  $\times$  100  $\times$  100 cm (length  $\times$  width  $\times$  height) made of thick Plexiglas sheets was employed. To simulate a free-field condition and decrease the wave's reflection effect, on both sides of the

**Fig. 2** Shaking table apparatus of the University of Tabriz

soil container box and perpendicular to the shaking direction, relatively compressible foam expanded polystyrene sheets with a thickness of 5 cm were used.

### 2.2 Scaling factor

In the experimental modeling, the first step is to determine the specification of the scaling laws. The scaling ratio plays a key role in having a reliable model and test results. Thus, the correct scaling law between the physical modeling and the prototype must be considered for scaling up the experimental results to prototypes. To insure the dependency of soil behavior on the stress level and the compatibility of ground motion properties with real earthquakes, scaling law should be satisfied in modeling. In this study, for the 1 g shaking table tests, the scaling factors were determined based on the similitude law suggested by Wood and Crewe [37]. The scaled parameters applied to the models are summarized in Table 2. There are some limitations in prototype modeling by 1 g shaking table tests. The shear strength and stiffness of soil depend on the effective stress. The stress levels in a small-scale model under earth's gravity (1 g model) were much lower than those in a real structure. Despite these limitations and based on previous studies, for discovering trends of soil-pile-foundation systems' seismic behavior, shaking table tests are very useful, giving fundamental information on the performance of the model [27]. Finally, according to the shaking table properties and model characteristics and other limitations, the geometric scale factor ratio was selected as 25.

**Table 2** Scaling factor for 1 g shaking table tests

Item	Notation	Wood and Crewe [37]	This study
		Prototype/model	Prototype/model
Length	$L$	N	25
Density	$\rho$	1	1
Shear modulus	$G$	$N^{0.5}$	5
Acceleration	$a$	1	1
Stress	$\sigma$	N	25
strain	$\varepsilon$	$N^{0.5}$	5
Displacement	$d$	$N^{1.5}$	125
Dynamic times	$t$	$N^{0.75}$	11.180
Frequency	$f$	$N^{-0.75}$	0.089
Shear wave velocity	$V_s$	$N^{0.25}$	2.236
Pile flexural rigidity	$EI$	$N^{4.5}$	1953125

### 2.3 Soil and CPRF properties

The soil under investigation in this research is No. 161 Firouzkooch sand, sourced from Firouzkooch county, Iran. Several previous studies have delved into both the static and dynamic properties of No. 161 Firouzkooch sand [38–40], with its utilization observed in various physical models as well [41, 42]. The particle size distribution and pertinent properties of the sand are depicted in Fig. 3 and detailed in Table 3. The effective stress friction angle of the soil corresponding to the targeted relative density was determined through direct shear tests. According to the Unified Soil Classification System (USCS), this sand falls into the category of poorly graded sand (SP). Although the usage of well-graded sand is customary in field applications, the uniformity of laboratory compaction is better attained with poorly graded sand.

Besides, as listed in Table 4, the concrete raft foundation was scaled to model as a rectangular box 25 cm × 25 cm × 4 cm (length × width × height), made of concrete connected to four vertical piles with a total length of 72 cm, where upper 2 cm was embedded in the concrete foundation to make sure a fixed connection. Piles were made of hollow bars of aluminum alloy of elastic modulus,  $E$ , equal to 70 GPa and density,  $\rho$ , equal to 27 kN/m<sup>3</sup> with outer 10 mm and inner 8.4 mm diameter installed in 125 mm center to center spacing founded on the top of a 50 cm height slope.

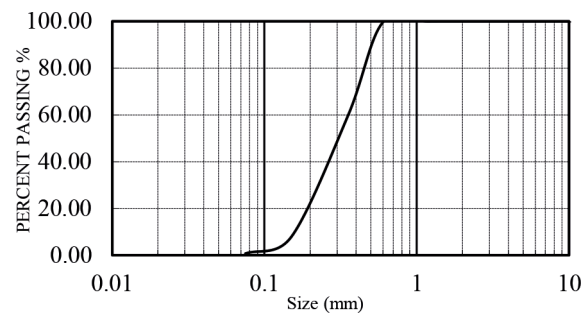


**Fig. 3** Grain size distribution graph of No. 161 dry Firouzkooch sand

**Table 3** Material properties of the No. 161 Firoozkuh sand

Item	Value
Density (kg/m <sup>3</sup> ) of 60% Dr	1550
G <sub>s</sub>	2.658
D <sub>50</sub> (mm)	0.23
C <sub>u</sub>	1.32
C <sub>c</sub>	0.92
$e_{max}$	0.886
$e_{min}$	0.637
Shear wave velocity (m/s)	160

**Table 4** Physical properties of structural elements

Structural element	Property	Model
Pile	Material	Aluminum
	Out diameter	10 mm
	Inner diameter	8.4 mm
	Thickness	0.8 mm
	Length	70 cm
	number	4
Raft foundation	Material	Concrete
	Width	25 cm
	Length	25 cm
	Thickness	4 cm

## 2.4 Model preparation and instrumentation

To model the soil medium, the soil mass was compacted to reach 60% of the maximum relative dry density ( $D_r$ ). In this way, the weight of compacted soil of each layer was calculated based on specific density that was presented in Table 3 and volume of each layer. Finally, 215 kg of dry No. 161 Firuzkooh sand for each step of filling the soil layer in a solid box were used. Then, in every step, the soil mass was compacted to reach finally 10 cm predicted constant height layer. The Soil box was filled by compacted 8 layers from bottom to top of the soil. The final soil model was 80 cm in height, 80 cm in width, and 173 cm in length. The soil used in these tests had an average moisture content of about 5%. The properties of the sand used in the experiments are summarized in Table 3. During model preparation, in every step, instruments including 5 accelerometers, 4 piles were placed in their predicted positions, simultaneously in the course of soil compaction progress. At the end, a raft foundation built of concrete with 4 predicted holes to fix piles heads in their cap, was placed on piles top. Finally, the models' length became 173 cm, with 81.5 cm for the slope top area and 91.5 cm for the slope body area. Also, the models' total height was 80 cm, 50 cm of which was allocated for the slope body and 30 cm for the slope bed. The models' slope angle was changed on every model to 0°, 30°, 45°, 60°, and 90°. To better describe, Fig. 4 depicted a schematic view of the model geometry and instruments. As mentioned above, five accelerometers (briefly A) with a precision of 0.01 g were placed in their positions to measure acceleration in various elevations of the model to calculate the amplification phenomenon (Fig. 4). To avoid container boundary effects, accelerometers used in soil mass were embedded sufficiently far from the container boundaries (Fig. 4 (a)). All of these instruments are connected to a device of dynamic signal

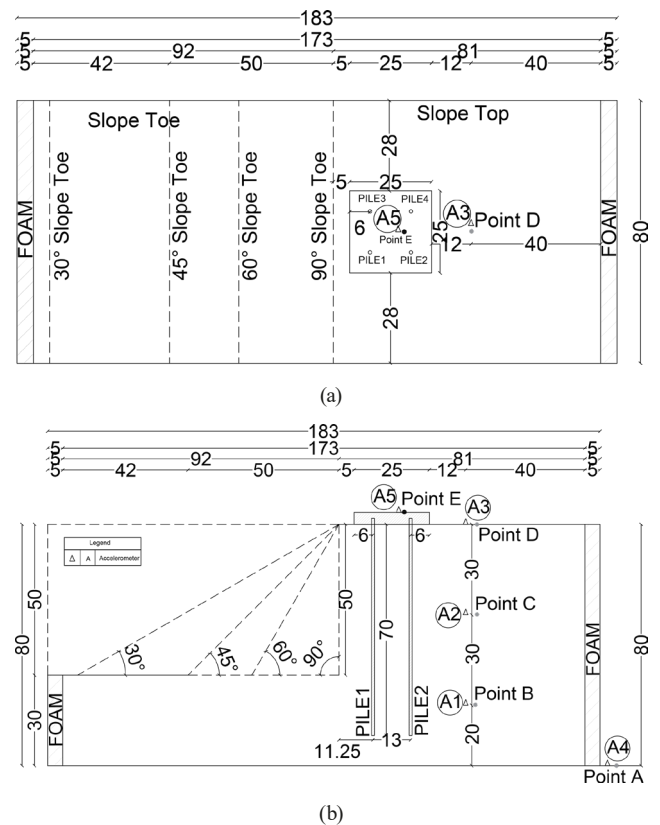


**Fig. 4** Schematic shaking table model with instruments location: (a) plan view, (b) elevation view

acquisition system utilized to collect data in 32 channels simultaneously. In this regard, Fig. 5 demonstrate prepared models of shaking table test before start of motion.

## 2.5 Input motions and loading characteristics

In seismic experimental studies, for better observation of the amplified response of the model, it is important to obtain the predominant frequency of the model due to vibration. In the present study, the procedure recommended by Gohl [43] was used to determine the predominant frequency. In this regard, white noise excitation with a frequency range of 0.1–50 Hz was applied to the model, and soil response as Fourier spectra at the base of the model and soil surface were computed from the recorded accelerations. Based on the results, for the flat ground model condition, the maximum Fourier amplitude occurred at a frequency of 6.86 Hz, while for the slopes with the angles of 30, 45, 60, and 90 degrees, it was about 6.12, 5.78, 5.32 and 5.17 Hz, respectively. For better investigation of the seismic response of the slope, it is imperative to select appropriate ground motion. In addition, the changes in normalized frequency  $H/\lambda$  defined as slope height  $H$  and wavelength  $\lambda$ , had a great effect on the seismic response of soil slope, as proven by previous studies [16].

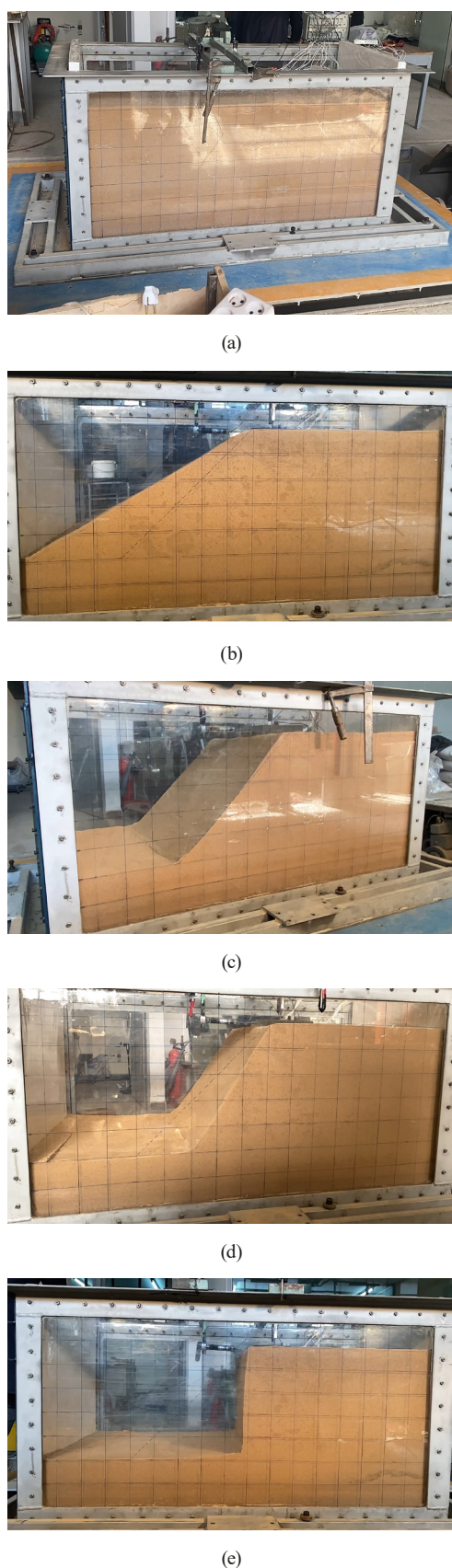


**Fig. 5** Prepared models based on shaking table with various slope angles before test: (a) flat ground, (b) slope of 30°, (c) slope of 45°, (d) slope of 60°, (e) slope of 90°

Since the acceleration magnitude play a key role in the evaluation of seismic response [7], the frequencies of input motions were selected as 3, 5 and 8 Hz, almost close to the predominant frequency range, and the acceleration of input excitations was selected as 0.35 g and 0.5 g. Considering the difficulties of analyzing the fundamental patterns of seismic behavior of physical models using complex input motions from real earthquake events, sine harmonic waves would be a good choice and were considered as the base excitation for these experiments. To simplify effective parameters in input motions, harmonic sinusoidal waves were proposed for this type of experiment. Finally, designed input motions were applied to the base of the shaking table model with 6-sec duration as 6 types of harmonic sinusoidal waves with a magnitude of the peak ground accelerations (PGA) of 0.35 g for moderate earthquakes, and 0.5 g for strong earthquakes consisting of constant frequency of 3, 5 and 8 Hz. Thus, a wide range of seismic motions as 3 Hz - 0.35 g, 5 Hz - 0.35 g, 8 Hz - 0.35 g, 3 Hz - 0.5 g, 5 Hz - 0.5 g, 8 Hz - 0.5 g, as input1 to input6, respectively, was applied to the model to achieve more useful outputs. In this regard, Fig. 6 shows the acceleration time histories and Fourier spectra of the harmonic input motions recorded by A4, the accelerometer placed at the base of the shaking table deck. As mentioned in Table 5, in this research, 59 shaking table tests were programmed to investigate the seismic response of CPRF located near a slope.

### 3 Tests program

#### 3.1 Tests description

To investigate the seismic response of the slopes under different conditions, 59 types of tests, according to Table 5, were programmed and conducted. As mentioned in the previous section, white noise excitation tests including Nos. 1 to 5 were carried out to obtain the predominant frequency, before the performance of the first test of each slope angle. Then, for every model with a certain slope angle, 6 types of sinusoidal harmonic waves as input excitations were applied to the model. Tests No. 6 to No. 11 tests were performed on the flat ground model and the data were gathered by instruments installed, which in the signals recorded a negligible deformation was seen on the soil surface. Then, No. 12 to No. 17 tests were done on the slope with a 30° angle and little deformation on soil crest was seen with some small cracks on the surface without any serious failure on the slope body. Next, tests No. 18 to No. 23 were carried out on the 45° slope model and

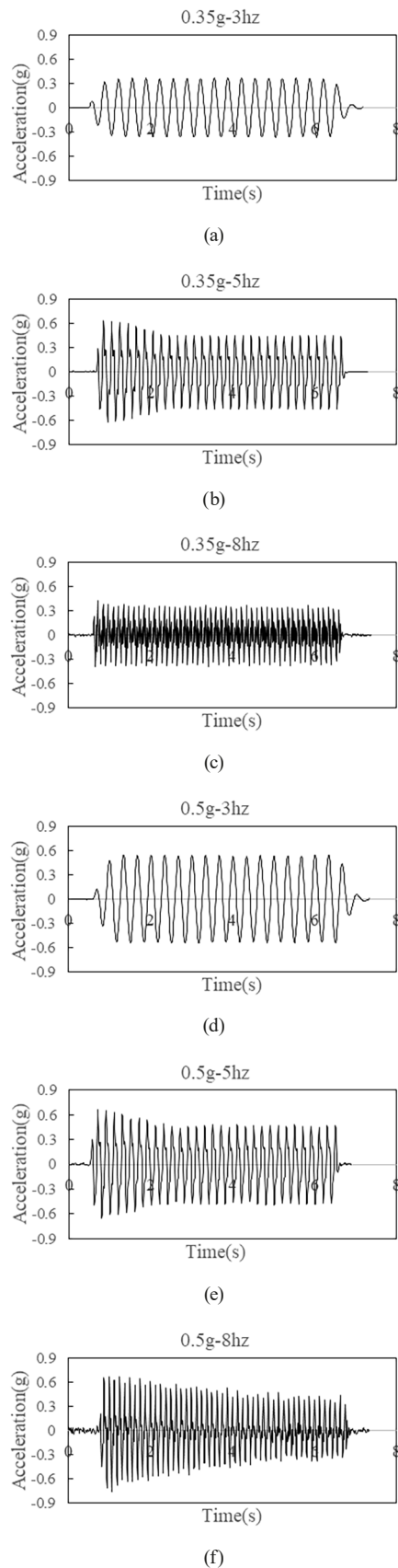


**Fig. 6** Time history of input motions obtained from A4: under motion of (a) Input1, (b) Input2, (c) Input3, (d) Input4, (e) Input5, (f) Input6

after the application of 5 types of motions; slope failed at 0.5 g - 5 Hz excitation motion, causing serious damage. After that, tests No. 24 to No. 29 were performed on the 60° slope model and the slope failed on 0.5 g - 3 Hz motion, after which other motions were not applied after failure. Finally, the selected motions were applied to a 90° slope as tests No. 30 to No. 35, among which only 0.35 g - 3 Hz and 0.35 g - 5 Hz tests were done, and 0.35 g - 8 Hz tests motions were applied after failure. In addition, to evaluate the effect of the non-use of piles on system seismic response, a series of tests were performed on flat ground and 45° slope, as tests No. 36 to No. 47. Also, to investigate the pile length effect, tests No. 48 to No. 59 were conducted on the model of slope 45°.

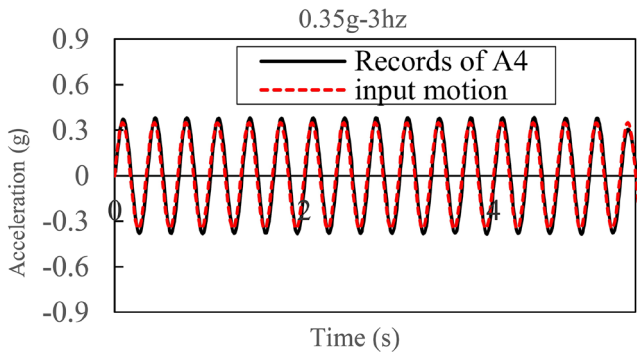
### 3.2 Consideration of acceleration records on the model

Fig. 7 shows the input excitations from the shaking table apparatus applied to the bottom of the table deck and acceleration received at the A4 accelerometer located on the table deck (elev. 0.00). As shown in Fig. 7, a negligible difference was encountered in both acceleration and frequency characteristics, demonstrating a good agreement between input and received data. To consider the effect of wave propagation on its characteristics in the soil mass, 3 other accelerometers, A1, A2, and A3 at elevations +20, +50, and +80 cm, respectively, were used. Besides, to investigate the raft foundation response due to the seismic excitations, another accelerometer was utilized as A5 on the top of the concrete foundation (elev. +84 cm) having a 17 cm horizontal distance from the slope crest. One of the suitable parameters, as a recognized index, which is widely used to describe seismic response is the amplification factor (AF), defined by the ratio of received motion PGA (Peak Ground Acceleration) at a special point to the input motion excited from the source point. In this regards, it is important to consider PGA in different situations. In this study, it was calculated from the ratio of selected accelerometers PGA to input motion (A4) PGA, the comprehensive results of which will be discussed in the subsequent sections. For precise analyses and comparison of received motions at each accelerometer, acceleration-time history records in this paper were selected from 2 to 3 seconds were selected in this study (Fig. 8).

For example, Fig. 8 shows the waves picked up by accelerometers in the test No. 18 (slope 45°, under 0.35 g and 3 Hz input motion). Considering Fig. 8, the PGA magnitude increased slightly at the location of A1 (point B), and more at A2 (point C). This variation was due to the wave

**Table 5** Experimental program of 1 g shaking table tests on CPRF model

Test No.	Wave form	Slope angle (degree)	Frequency (Hz)	PGA (g)	Pile	Model description
01–05	White noise	0 to 90	0.2–50	0.05	✓	Natural frequency of vibration
06–11	sine	0 (flat)	3, 5, 8	0.35, 0.5	✓	CPRF on slope crest (slope angle, acceleration and frequency of dynamic excitation was various)
12–17	sine	30	3, 5, 8	0.35, 0.5	✓	
18–23	sine	45	3, 5, 8	0.35, 0.5	✓	
24–29	sine	60	3, 5, 8	0.35, 0.5	✓	
30–35	sine	90	3, 5, 8	0.35, 0.5	✓	
36–41	sine	0 (flat)	3, 5, 8	0.35, 0.5	×	
42–47	sine	45	3, 5, 8	0.35, 0.5	×	
48–53	sine	45	3, 5, 8	0.35, 0.5	✓	Piles length 60 cm
54–59	sine	45	3, 5, 8	0.35, 0.5	✓	Piles length 50 cm



**Fig. 7** A sample of acceleration time history of induced input motion of shaking table in comparison with recorded data at A4

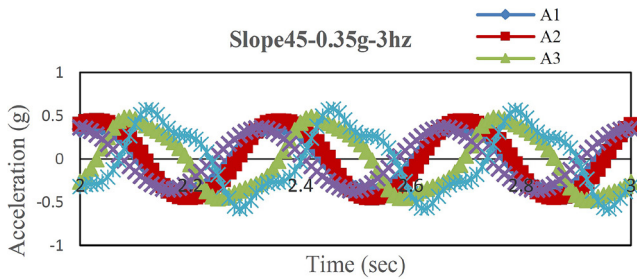


**Fig. 8** Acceleration time history of recorded data at 5 accelerometers that was used in No. 18 test

propagation in the soil mass and its effect on wave velocity and acceleration properties. At A3 which is located on the soil surface, waves were received with higher peak amount and therefore, more amplification was concluded respectively. In addition, A5 experienced more amount of acceleration compared to A3, probably because of its closer distance to the slope crest and reflected waves from the slope surface. It was observed that the peak points of the curves (PGA) were different at accelerometers since wave propagation in the soil mass and amplification phenomena was considerable.

### 3.3 Distribution patterns of the PGA of the slope

According to previous studies, a parameter  $H_{cr}$  is employed as the critical height of the slope in order to distinguish a border for the slopes' seismic behavior. It is defined as a function of the geometry of the slope, soil, and input excitation parameters of the system.

Qi et al. [13] concluded that the critical height of the slope could be expressed as approximately one-fifth of the wavelength of the dynamic input motion, varying in the range of 0.17–0.21, as shown in Eqs. (1) and (2).

$$H_{cr} = (0.17 \sim 0.21)\lambda \quad (1)$$

$$\lambda = \frac{V_s}{f} \quad (2)$$

$$\begin{cases} H \geq H_{cr} & \text{dynamic response of slope takes} \\ & \text{on high slope dynamic response} \\ H \leq H_{cr} & \text{dynamic response of slope takes} \\ & \text{on low slope dynamic response} \end{cases} \quad (3)$$

According to Eq. (3), slope height ( $H$ ) can be compared with the critical height, as  $H \geq H_{cr}$  which means that the dynamic response of the slope takes on a high dynamic response and vice versa. In this study, considering the shear wave velocity, frequency, and slope height of about 150 m/s, 3, 5, 8 Hz, and 50 cm, respectively, the corresponding shear wavelengths became about 50, 30, and 18 m, determined by Eq. (2). According to Eq. (1), the critical heights  $H_{cr}$  of the slope for the shaking table tests with different waves were about 10, 6 and 3 m, respectively, higher than the height of the slope. Hence, the dynamic response of the slope would exhibit a low slope dynamic response. Based on Fig. 9, there were two types of distribution patterns of the AF of the



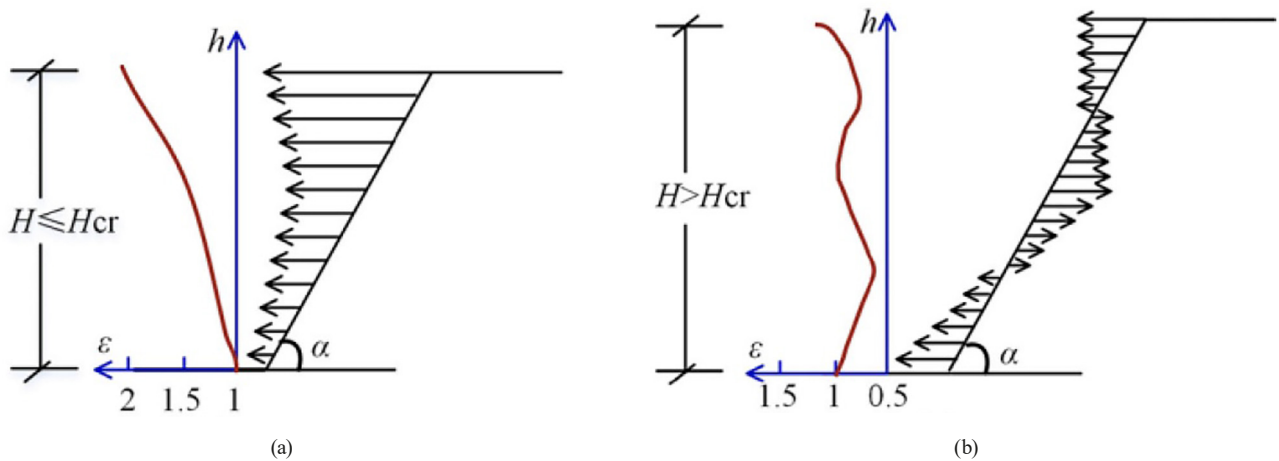


**Fig. 9** Two different patterns of amplification in which particle vibration mode along the slope surface is different: (a) low slope dynamic response,  $H \leq H_{cr}$  and (b) high slope dynamic response,  $H > H_{cr}$  [13]

slope. In the present study, considering  $H < H_{cr}$ , the results confirmed the pattern of Fig. 9 (a). Comparison of AF along soil depth for different seismic excitations between flat ground with CPRF model and foundation without pile model is presented in Fig. 10. As demonstrated in Fig. 11, the AF increased with increasing slope elevation similar to pattern of Fig. 9 (a).

## 4 Results

### 4.1 Foundations based on flat ground field

As mentioned above, the amplification factor was affected by the mass properties through which the wave was propagated. When piles were used to enhance the seismic performance of foundations, they affected the amplification ratio. To closer review, two types of flat ground surface models with CPRF and foundation without pile were made and the tests No. 36 to No. 41 were done. As shown in Fig. 10, the red line represented the AF on the CPRF model and the black line was referred to the model without pile. By investigating data and graphs, in the model with CPRF, on points B and C, a slight decrease in amplification factor was seen in comparison to that without the pile model, due to the close position of accelerometers to the excitation source. These results were approved by previous studies [27]. In Addition, on the soil surface (point D), in the model without pile, a few more AF, 3% on average, was calculated compared with the CPRF model. However, the AF increased with height in both cases, a typical elevation amplification effect. In addition, considering the model without a pile, on top of the foundation (point E), the increase of AF was more distinct, where AF under 0.35 g and 0.5 g excitation on point E was about 8% and 30% more compared to the model with CPRF. This result

showed that using CPRF in flat grounds decreased the amplification factor a little on the soil surface and much more on the foundation, causing a better seismic response in comparison with the foundations without a pile.

### 4.2 Influence of piles on seismic response of foundations placed near the slope crest

To investigate the effect of topography on the seismic behavior of CPRF and comparison with the foundation without a pile, another two models with a slope of  $45^\circ$  angle were established. In these models, foundations were located at the edge of the slope crest. No. 18 to 23 tests for the CPRF model and No. 42 to 47 for the model with pile-less foundation were done and data derived as graphs are shown in Fig. 11. These graphs show the distribution of horizontal acceleration amplification along the height of soil mass under seismic excitations including various accelerations and frequencies, as shown in Table 5 previously. In these graphs, the normalized elevation was calculated as  $h/H$ , where  $H$  and  $h$  refer to total height and accelerator location height from the deck bottom, respectively. The red line represented the AF on the CPRF model and the black line referred to the model without pile. Firstly, in both models, it was common in all graphs that in the higher soil level, more AF occurred. Besides, in the model with CPRF compared to that without pile, in the bottom of the model (point B), a slight change in AF from input motion amount was seen on both of them; however, while moving upward in soil mass (point C) to the soil surface (point D), some more AF change was observed. In previous studies conducted by Zhu et al. [44] and Qi et al. [13], an amplification along the height of slope was observed, confirming the reliability of our results obtained by the shaking

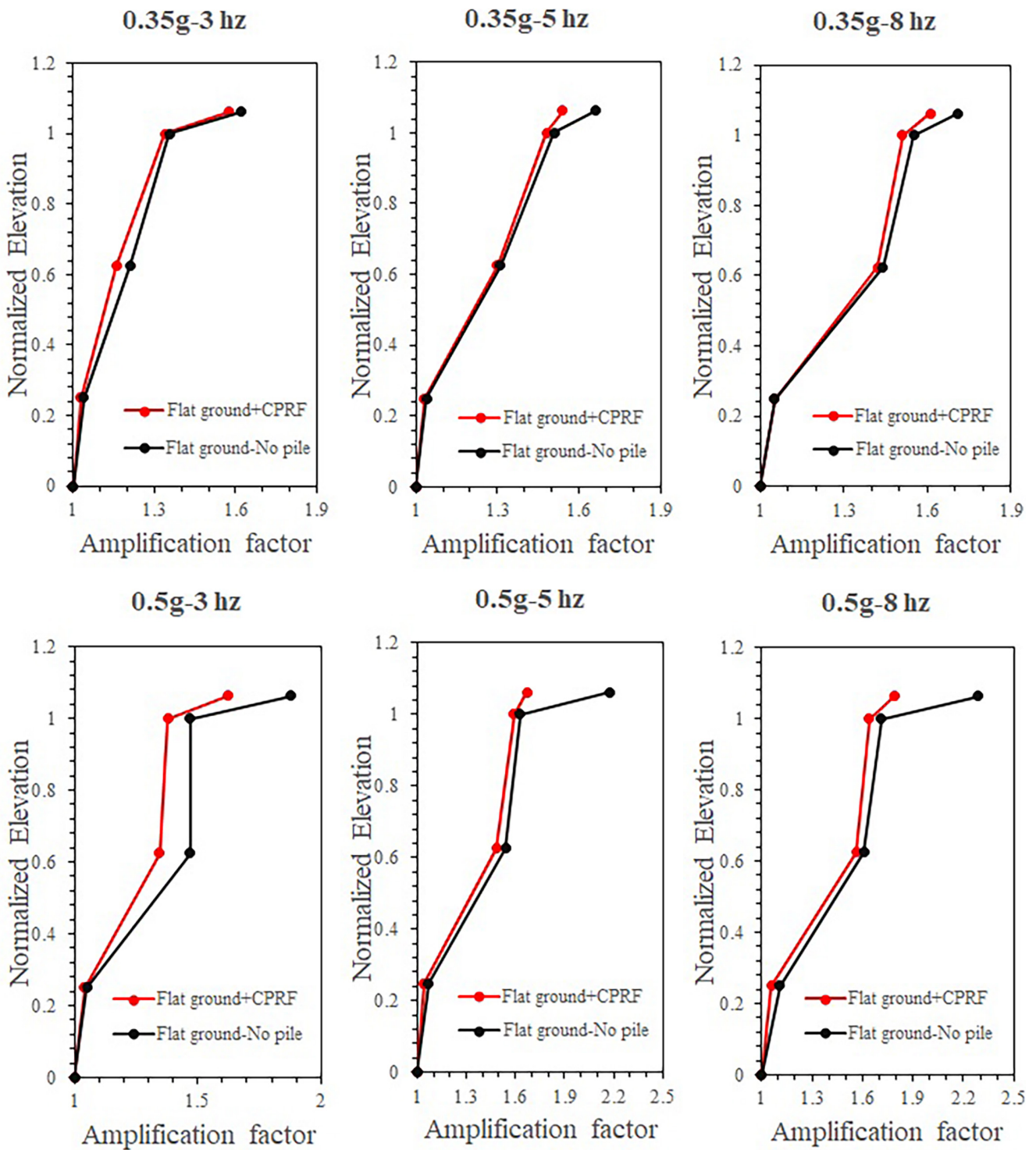


**Fig. 10** Comparison of AF along soil depth for different seismic excitations between flat ground with CPRF model and foundation without pile model

table tests. Therefore, using the CPRF on the slope crest led to about an 11% to 16% decrease in the acceleration amplification on the soil surface compared to the model without a pile. It was noteworthy that the highest effect of using pile was observed on foundation response (point E), while AF decreased about 20% to 27% on the model with CPRF. In addition, under stronger motions, the effect of

using a pile on AF was considerable. Secondly, as shown in Fig. 12, on the foundation without a pile compared with the CPRF model, much more displacement and a larger failure surface were observed. Additionally, the presence of piles under the foundation built near the slope crest prevented it from collapsing and it was stable despite emptying the soil under the foundation. Therefore, it was evident

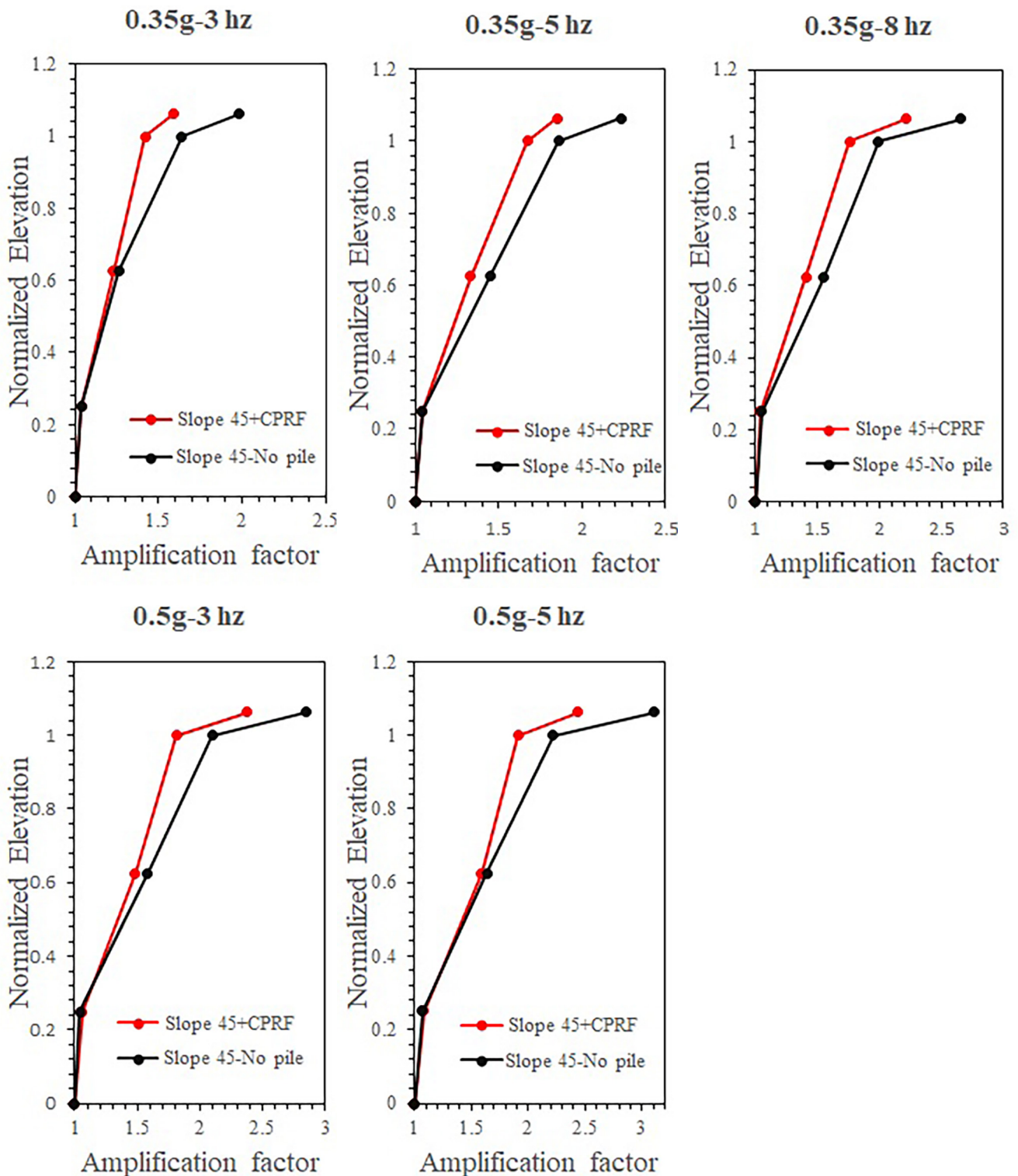
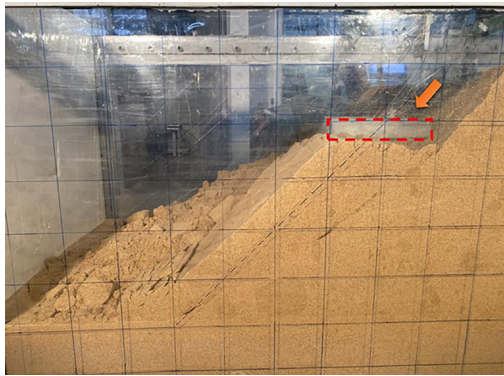


Fig. 11 Comparison of AF along soil depth for different seismic excitations between slope of  $45^\circ$  with CPRF model and foundation without pile model

that using a pile made foundation safer on the slope crest. Furthermore, considering the slope  $45^\circ$  model, the AF had more amounts in comparison with the flat ground model, owing to the topography effect on the seismic response of the system. This increase in AF was due to wave reflection effect near the slope crest and wave travel path from

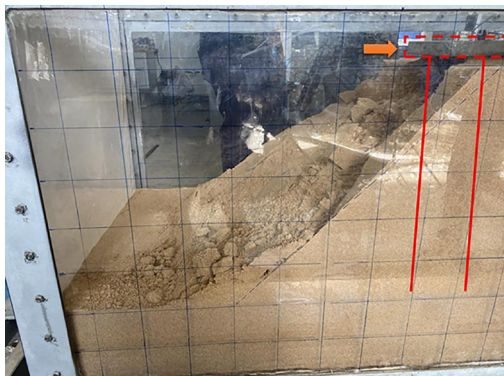
the source to accelerometers' locations. As a result, using pile caused a decrease in AF up to about 15% on the soil surface and about 25% on the foundation, resulting in better seismic response and stability of the foundations near slope crest. In this regard, according to Fig. 12, in the slope of  $45^\circ$  without piles, the foundation collapsed and moved



(a)



(b)



(c)



(d)

**Fig. 12** Comparison of deformation of soil mass after failure of 45° slope, (a) side view and (b) top view of model of without pile foundation, (c) side view and (d) top view of CPRF model

downward due to dynamic loads and at the same time the slope crest failed and experienced severe damage as a full landslide. On the contrary, in the model with piles, the foundation remained stable and piles prevented a full landslide. However, in this model, the slope was damaged with limited local destruction.

#### 4.3 Influence of piles length

As mentioned above, the foundations built in the vicinity of the slope crest were more subjected to major displacement and failure under severe earthquakes, making it necessary to use piles to prevent their moving in those areas. In this section, the effect of pile length is investigated. For a better conclusion, 3 types of piles with different lengths were used. The models were only different in pile length while being similar in the slope angle and other properties and instruments. The slopes' angle was 45° and the pile lengths were 70, 60, and 50 cm according to Table 5. The related tests under 6 types of input motions, as tests No. 48 to No. 59, were done.

The data obtained from accelerometers and their related AF is summarized in Fig. 13, for various input motions. Based on the results in Fig. 13, for point B, the increase in input acceleration and pile length did not have a considerable effect on AF. Next, the results showed that the decrease of pile length, limited to slope height, did not have a great effect on changes of the AF at points C and D considering certain slope angles. But in point E, it was observed that the increase in pile length led to a decrease in AF. Under stronger motions, AF growth due to using short piles was clear and in the model with pile 50 cm, the increase was more noticeable. Finally, it could be concluded that the pile length had a great effect on CPRF seismic response and a little effect on the acceleration of the soil mass and the soil surface on the slope.

#### 4.4 Slope angle effect on seismic response of slope-CPRF system

In this section, the effect of slope angle was investigated. For a better conclusion, 5 types of topography-changed models were used. The models were only different in the slope angle and similar in other properties and instruments. The slopes' angles were 0 (as flat ground), 30°, 45°, 60° and 90°, and according to Table 5, the related tests under 6 types of input motions, as tests No. 6 to No. 35, were done. The data derived from the accelerometers and their related AF is summarized in Fig. 14 (points B to E) graphs, for various input motions, respectively.

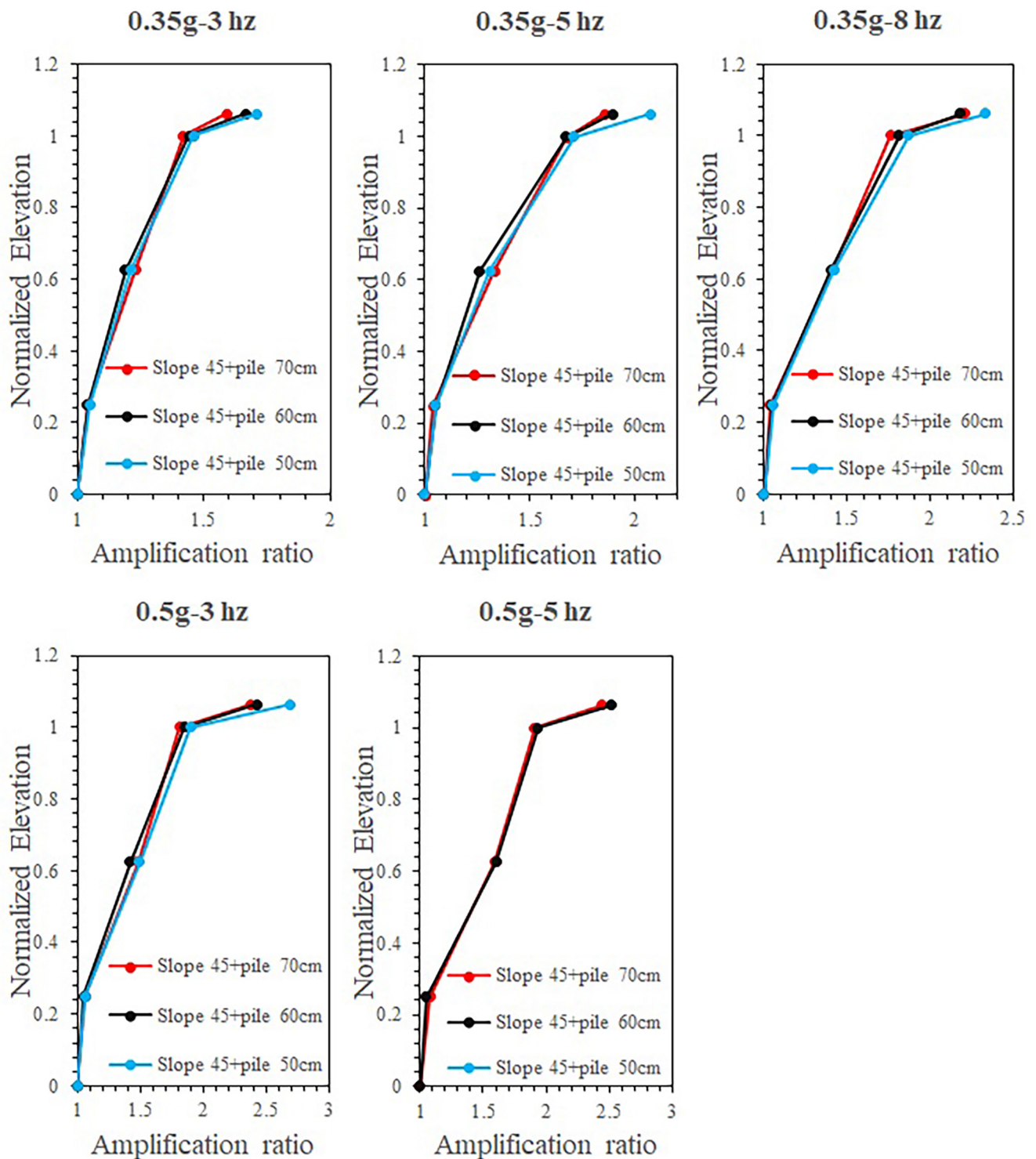
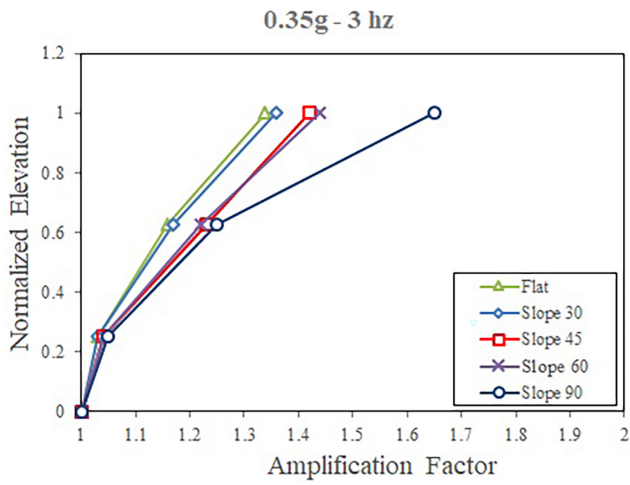


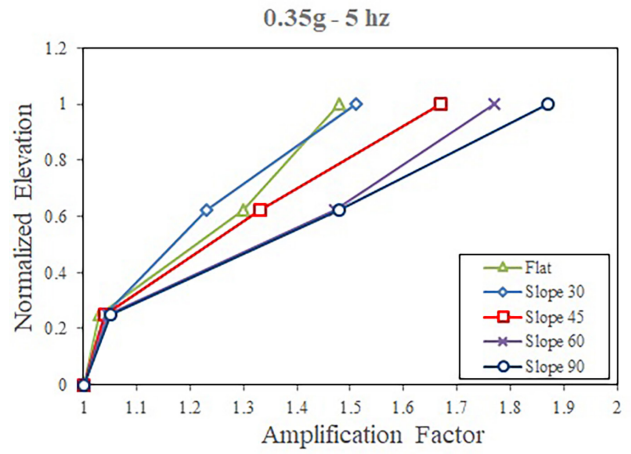
Fig. 13 Comparison of amplification factor along soil depth of slope of 45° model for different pile length and for various seismic excitations

It is noteworthy that, in the input motion with 0.5 g acceleration compared with 0.35 g, less number of tests could be performed because of slope failure occurring in previous tests. Based on the results in Fig. 14 for point B (bottom of soil mass), an increase in input acceleration and soil slope angle resulted in a slight increase in AF. Next, considering the seismic response of the soil in point C in

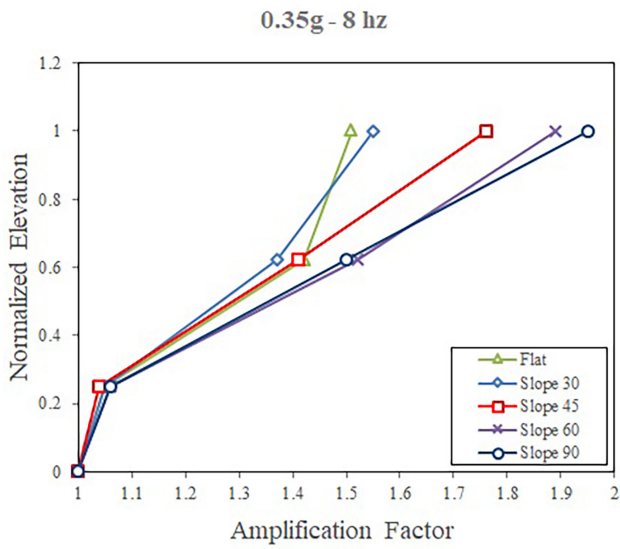
constant frequency and a certain slope angle, an increase in the input acceleration led to more growth in AF, while in flat ground, 30° and 45° slope models, this increase was less noticeable. Besides, the increment rate was greater in 60° and 90° slopes. In addition, the soil on point D experienced much more AF than other previous points.



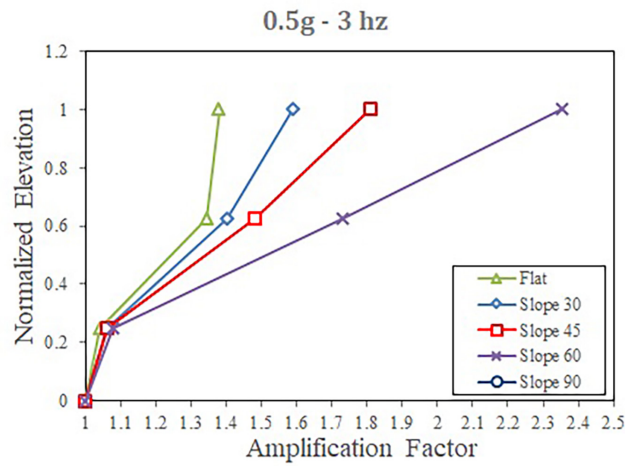
(a)



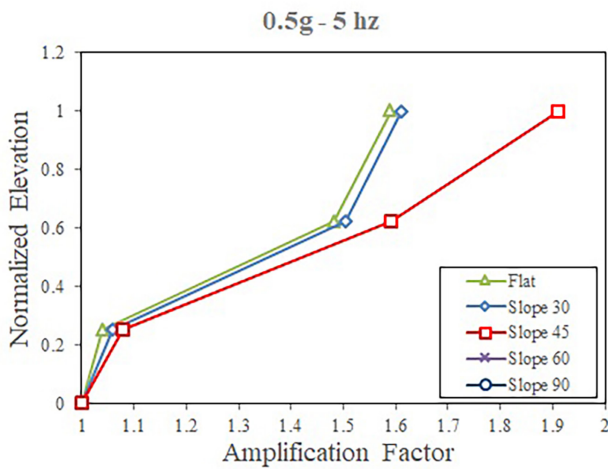
(b)



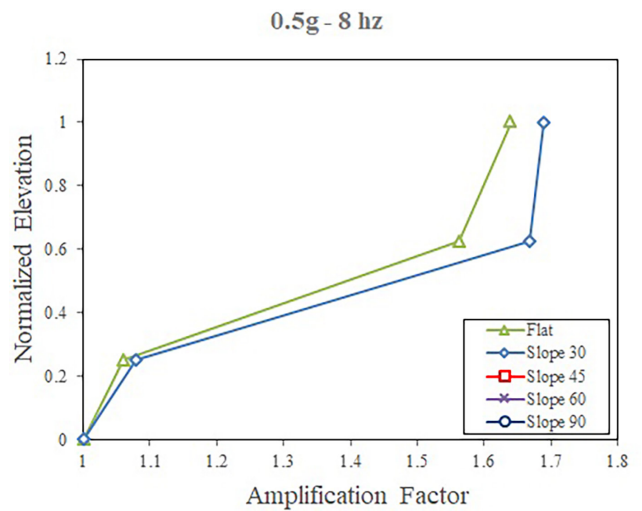
(c)



(d)



(e)



(f)

**Fig. 14** Effect of slope angle on the amplification factor at different points of slope for various seismic excitations: (a) Input1, (b) Input2, (c) Input3, (d) Input4, (e) Input5, (f) Input6

In point D, the growth of AF due to the increase in slope angle was evident. Under the excitation of 0.35 g, for the flat ground model, AF was about 1.34 to 1.51, for the 30° slope, it was from 1.36 to 1.55 for the slope 45°, it was from 1.42 to 1.76 and for the slopes 60° and 90°, it ranged between 1.44 to 1.89 and 1.65 to 1.95, respectively. The AF had more amounts when the model was subjected to 0.5 g motion and the maximum value of AF reached 1.64 for the flat ground, 1.69 for the 30° slope and 1.91 and 2.35 for the slopes 45° and 60°, respectively. This range of AF for various slope angles proved the prominent effect of slope angle on the acceleration amplification on the soil surface of the slope crest. At all slope angles, the amount of AF in point E was more than that in point D i.e. while the amount of AF for motion 0.35 g in point D was from 1.33 to 1.95, for point E, it was between 1.56 and 2.5, probably because of two main reasons: Firstly, the interaction between soil topography-structure and secondly more distance of point D from the crest of the slope in comparison with point E. Above all, on point E, the most AF occurred. The AF measured on the foundation located on the flat ground was from 1.54 to 1.61 under 0.35 g excitation and 1.62 to 1.79 under 0.5 g motions; while in the slopes, it varied from 1.56 for 30° slope to 3.07 for 60° slope, showing a great increase because of topographic irregularities. Furthermore, the percentage of growth of AF on point E for the motion 0.5 g compared to 0.35 g motion, for the flat ground was about 10%, for the 30° slope about 35%, and for the slope with 45° angle about 50%, while in the only test of 60° slope under 0.5 g motion, about 85% increase was seen. This increase confirmed the considerable effect of the slope angle on the AF of superstructures near the crest i.e. AF was more effective in stronger motions. Additionally, the frequency increase in points D and E had a greater effect on AF compared with points B and C, and it was noteworthy that the effect of the frequency increase was more remarkable on 60° and 90° slopes, discussed in the next paragraph. As a result, in stronger earthquakes, constructions on a steep slope crest experience more amplified motions and this must be noticed in their designing criteria. Finally, it could be summarized that in steeper slopes and under stronger motions, amplification was more substantial and should be seriously considered. Table 6 presents all of the accelerations have read by accelerometers on all tests.

#### 4.5 Seismic response of slope-CPRF system

To better understand the excitation motion effect on the seismic response of slopes, Fig. 15 was investigated. Fig. 15 plots the AF along the height of the model for different

**Table 6** Summary of PGA of selected points in various slope angles

Slope	Point	Input1	Input2	Input3	Input4	Input5	Input6
0	B	0.360	0.360	0.367	0.520	0.521	0.53
0	C	0.406	0.455	0.497	0.672	0.741	0.781
0	D	0.469	0.518	0.528	0.691	0.795	0.82
0	E	0.551	0.539	0.563	0.567	0.584	0.626
30	B	0.361	0.364	0.367	0.530	0.532	0.54
30	C	0.409	0.430	0.479	0.701	0.753	0.834
30	D	0.476	0.528	0.542	0.695	0.805	0.845
30	E	0.546	0.605	0.658	1.061	1.130	1.175
45	B	0.364	0.364	0.364	0.53	0.54	0
45	C	0.430	0.465	0.493	0.74	0.795	0
45	D	0.497	0.584	0.616	0.905	0.955	0
45	E	0.556	0.647	0.773	1.19	1.220	0
60	B	0.364	0.365	0.371	0.54	0	0
60	C	0.427	0.514	0.532	0.864	0	0
60	D	0.504	0.619	0.661	1.177	0	0
60	E	0.581	0.819	0.868	1.535	0	0
90	B	0.367	0.367	0.371	0	0	0
90	C	0.437	0.518	0.525	0	0	0
90	D	0.577	0.654	0.682	0	0	0
90	E	0.623	0.841	0.875	0	0	0

seismic excitations in different slope angles (A1 to A3 and A5 in Fig. 4 (b)). The graphs showed an additive trend for AF along the model height and especially this trend was remarkable on top of the CPRF. Besides, considering each slope's angle, the more frequency caused more AF.

Additionally, this increment was observed when the model experienced more input PGA. So, the stronger excitation led to more AF in all slope angles. For precise investigation, the soil surface and top of the CPRF were discussed. The range of AF was different in the slope angles. On the flat ground model under medium motions (0.35 g), a sudden increase was observed on the soil surface point between input 1 and input 2 motions. This jump was seen on input 2 for the slopes of 30° and 45° and input 3 for the slope of 60°, respectively. As mentioned before, because of failure, strong motions were not applied to steep models of 60° and 90°, therefore, this sudden jump on AF could not be considered properly. One of the reasons for this sudden increase was the predominant frequency of each model and a similar period of model and motion could cause this type of jump on AF.

#### 4.6 Influence of normalized frequency on seismic response of model

As reported in previous papers, the normalized frequency ( $H/\lambda$ ) was used to evaluate the effect of frequency of motion on the seismic response of slope [16]. In this way, to reach

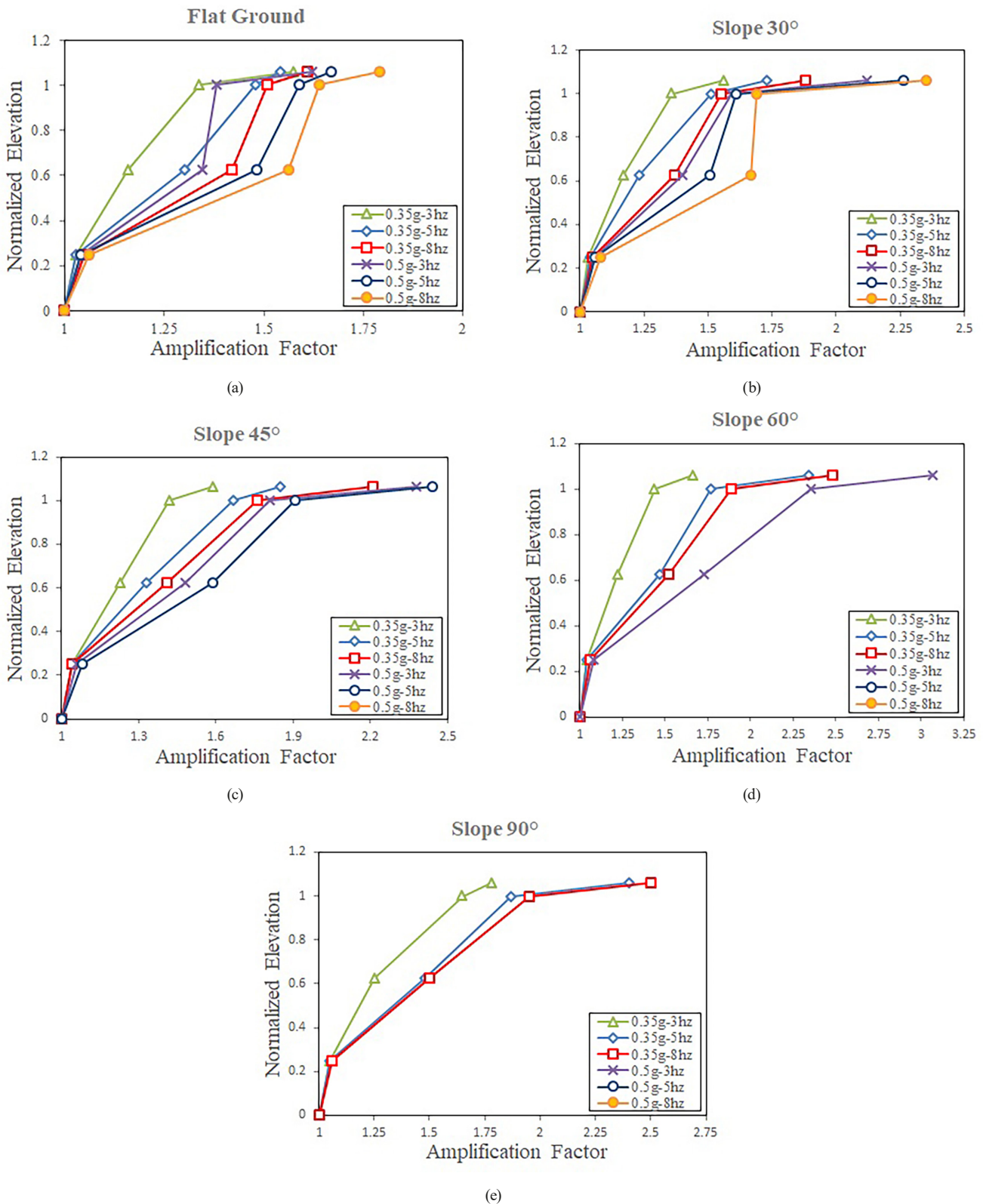


**Fig. 15** Comparison of AF along height of model for different seismic excitations in different slope angles: (a) flat ground, (b) slope of 30°, (c) slope of 45°, (d) slope of 60°, (e) slope of 90°

these parameters,  $H$  as slope height and  $\lambda$  as the wavelength for three types of waves were calculated and  $H/\lambda$  as 0.01, 0.016, to 0.026 was used in this study. However, based on Qi et al. [13], the AF at the crest of the slope

increased with increasing the normalized frequency ( $H/\lambda$ ) when  $H/\lambda$  was less than 0.17–0.20.

In addition, when  $H/\lambda$  was greater than about 0.17–0.20, the AF would decrease and de-amplification at the crest



occurred especially when  $H/\lambda$  was over 0.4. In this order, because of the limited height of the shaking table model and failure occurring on most of the slopes under intense motions, a wide range of excitations was not possible to apply, the limitation forcing the model to behave as low slope dynamic response. In summary, in this study, an increase in AF was expected. Fig. 16 demonstrates the AF versus  $H/\lambda$  under various slope angles for a constant slope height  $H$ . In general, depending on the slope angle and the frequency of the input motion wave and its intensity, different slope responses could be expected. In the acceleration of 0.35 g, the increase in the rate of the AF in the first changes of the input motion, and an increase in the frequency from 3 Hz to 5 Hz at the angles of  $60^\circ$  and  $90^\circ$

was more compared to other angles; with an increase in the frequency from 5 Hz to 8 Hz, the increasing rate of AF decreases. Also, the AF increase in 8 Hz input motion was greater than that in 3 Hz and 5 Hz. Therefore, it could be concluded the horizontal acceleration amplification factor under the motions with more frequency was more remarkable. For precise investigation, point D as the soil surface and point E on top of the foundation were considered. AF at point D increased a lot with the increase in the  $H/\lambda$  at the beginning, subsequently growing gradually to reach its largest value. This phenomenon was roughly the same for point E; the larger AF at the slope crest occurred with the larger slope angle. These results were confirmed by previous studies [8, 13].

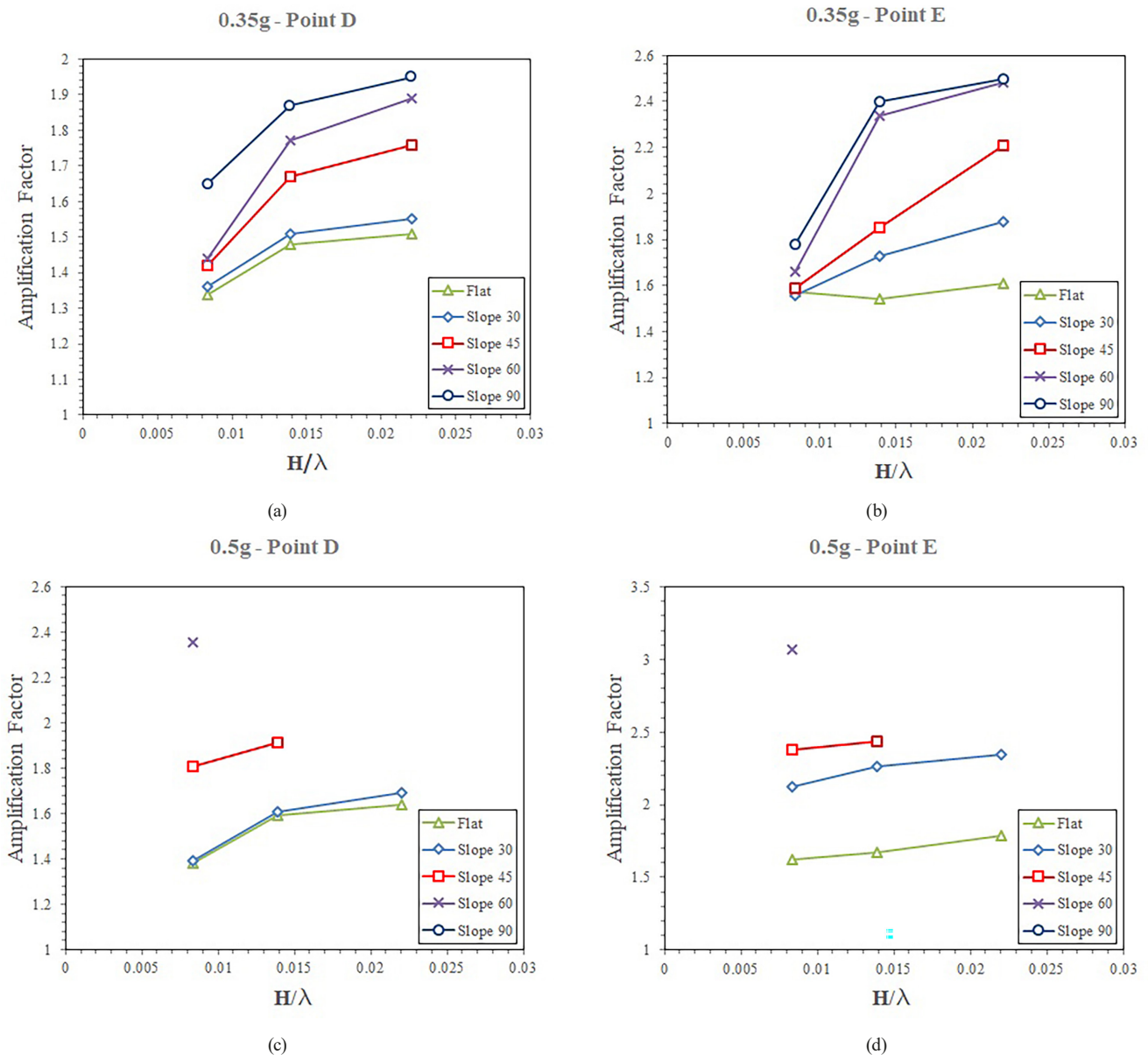


**Fig. 16** Comparison of AF distribution versus normalized frequency ( $H/\lambda$ ) for different slope angles in points D and E for 6 types of motion: (a) soil surface under moderate motion, (b) top of foundation under moderate motion, (c) soil surface under strong motion, (d) top of foundation under strong motion

#### 4.7 Amplification factor reviews on seismic codes

Soil topography amplification (ST) for the structures located in the vicinity of a slope was considered in the seismic design codes. For example, in the Iranian seismic code (Standard No. 2800) [26], similar to Eurocode8 (2008, cited in [13:p.12]) and NTC08 (2008, cited in [13:p.12]),  $ST > 1.4$  should be used for the slopes angle  $>30^\circ$  near the slope crest. In this study, considering the height of the slope less than  $H_{cr}$  and according to the results of previous studies [13], the seismic response of the slope was classified as low slope dynamic response. The results indicated for a system with sandy soil, the maximum value of ST reached about 2.35 and 3 on soil surface and top of foundation, respectively and the existing codes or provisions might underestimate the seismic response of the slope. It is noteworthy that the results and conclusions were obtained under harmonic wave motions.

#### 5 Future suggestions

This paper attempts to demonstrate that the presence of piles can reduce the amplification by comparing the amplification factors of foundations with and without piles using a small-scale shake table model to open a window for further and more comprehensive experimental and numerical researches. In models of this study, a dry standard granular soil has used while the other type of soils with various properties can be investigated. Also, the effect of saturation of underground layers on the seismic behavior of the slope which may lead to liquefaction, can be considered. Additionally, the effect of foundation distance to the edge of slope crest is one of engineering concern which can be studied experimentally and may led to some limitations in future Codes, for the CPRFs.

#### 6 Conclusions

In this study, a series of shaking table tests were conducted to study the effect of input PGA, frequency, and slope angle on the PGA of slope-CPRF system responses. The seismic behavior of the model was monitored by

instruments to investigate the seismic responses of the foundation and soil in the slope crest. According to the experimental results and detailed analyses, the main conclusions were made as follows:

1. Considering the amplification factor, using piles caused a little decrease on the AF in the flat ground soil medium and the soil surface while leading to a 30% decrease of AF on the top of the foundation.
2. Regarding the slope of  $45^\circ$ , using piles resulted in a decrease of AF up to about 15% on the soil surface and about 25% on the foundation, leading to better seismic response, less displacement, and stability of the foundations near the slope crest.
3. In general, the range of amount of AF for various slope angles proved the prominent effect of slope angle on the acceleration amplification on the soil surface of the slope crest, indicating that more slope angle caused more acceleration on the soil surface on the slope crest compared to the flat ground model. Therefore, it could be noteworthy for constructions on the slope crest and the necessity of more considerations in this regard.
4. The results confirmed that the slope angle had a great effect on the AF of superstructures near the crest and that AF was more effective in stronger motions.
5. In all models with various angles of slope, the increase of AF was more obvious under strong motions than moderate ones, on the soil surface and foundation.
6. The results approved that on the slope crest, the AF on the top of foundation had greater amount than soil surface.
7. It is observed that using shorter piles led to increase of AF on the top of foundation and failure occurred under weaker motions compared to longer piles.
8. Considering that  $H/\lambda$  is in a range that is below  $0.20 \lambda$ , and this causes the amplification factor to increase with the increase of  $H/\lambda$  and the de-amplification phenomenon is not observed in low slope dynamic response.

#### References

- [1] Day, R. W. "Design and repair for surficial slope failures", *Practice Periodical on Structural Design and Construction*, 1(3), pp. 83–87, 1996.  
[https://doi.org/10.1061/\(ASCE\)1084-0680\(1996\)1:3\(83\)](https://doi.org/10.1061/(ASCE)1084-0680(1996)1:3(83))
- [2] Fatahi, B., Huang, B., Yeganeh, N., Terzaghi, S., Banerjee, S. "Three-dimensional simulation of seismic slope–foundation–structure interaction for buildings near shallow slopes", *International Journal of Geomechanics*, 20(1), 04019140, 2020.  
[https://doi.org/10.1061/\(ASCE\)GM.1943-5622.0001529](https://doi.org/10.1061/(ASCE)GM.1943-5622.0001529)
- [3] Shabani, M. J., Ghanbari, A. "Comparison of seismic behavior of steel building adjacent to slope topography by considering fixed-base, SSI and TSSI", *Asian Journal of Civil Engineering*, 21(7), pp. 1151–1169, 2020.  
<https://doi.org/10.1007/s42107-020-00266-8>
- [4] Bahuguna, A., Firoj, M. "Numerical simulation of seismic response of Slope–Foundation–Structure interaction for mid–rise RC buildings at various locations", *Structures*, 44, pp. 343–356, 2022.  
<https://doi.org/10.1016/j.istruc.2022.08.011>

- [5] Gazetas, G., Kallou, P. V., Psarropoulos, P. N. "Topography and soil effects in the  $M_s$  5.9 Parnitha (Athens) Earthquake: The case of Adámes", *Natural Hazards*, 27(1–2), pp. 133–169, 2002.  
<https://doi.org/10.1023/A:1019937106428>
- [6] Assimaki, D., Gazetas, G., Kausel, E. "Effects of local soil conditions on the topographic aggravation of seismic motion: parametric investigation and recorded field evidence from the 1999 Athens earthquake", *Bulletin of the Seismological Society of America*, 95(3), pp. 1059–1089, 2005.  
<https://doi.org/10.1785/0120040055>
- [7] Zhang, C., Jiang, G., Lei, D., Asghar, A., Su, L., Wang, Z. "Large-scale shaking table test on seismic behavior of anti-slide pile-reinforced bridge foundation and gravel landslide: a case study", *Bulletin of Engineering Geology and the Environment*, 80(2), pp. 1303–1316, 2021.  
<https://doi.org/10.1007/s10064-020-02006-3>
- [8] Shabani, M. J., Shamsi, M., Zakerinejad, M. "Slope topographic impacts on the nonlinear seismic analysis of soil-foundation-structure interaction for similar MRF buildings", *Soil Dynamics and Earthquake Engineering*, 160, 107365, 2022.  
<https://doi.org/10.1016/j.soildyn.2022.107365>
- [9] Zhang, Z., Wang, T., Wu, S., Tang, H., Liang, C. "Seismic performance of loess-mudstone slope by centrifuge tests", *Bulletin of Engineering Geology and the Environment*, 76(2), pp. 671–679, 2017.  
<https://doi.org/10.1007/s10064-015-0846-2>
- [10] Hailemikael, S., Lenti, L., Martino, S., Paciello, A., Rossi, D., Mugnozsa, G. S. "Ground-motion amplification at the Colle di Roio ridge, central Italy: a combined effect of stratigraphy and topography", *Geophysical Journal International*, 206(1), pp. 1–18, 2016.  
<https://doi.org/10.1093/gji/ggw120>
- [11] Zhang, Z., Wang, T., Wu, S., Tang, H., Liang, C. "Seismic performance of loess-mudstone slope in Tianshui–Centrifuge model tests and numerical analysis", *Engineering Geology*, 222, pp. 225–235, 2017.  
<https://doi.org/10.1016/j.enggeo.2017.04.006>
- [12] Ding, Y., Wang, G., Yang, F. "Parametric investigation on the effect of near-surface soil properties on the topographic amplification of ground motions", *Engineering Geology*, 273, 105687, 2020.  
<https://doi.org/10.1016/j.enggeo.2020.105687>
- [13] Qi, S., He, J., Zhan, Z. "A single surface slope effects on seismic response based on shaking table test and numerical simulation", *Engineering Geology*, 306, 106762, 2022.  
<https://doi.org/10.1016/j.enggeo.2022.106762>
- [14] Li, Y., Wang, G., Wang, Y. "Parametric investigation on the effect of sloping topography on horizontal and vertical ground motions", *Soil Dynamics and Earthquake Engineering*, 159, 107346, 2022.  
<https://doi.org/10.1016/j.soildyn.2022.107346>
- [15] Tripe, R., Kontoe, S., Wong, T. K. C. "Slope topography effects on ground motion in the presence of deep soil layers", *Soil Dynamics and Earthquake Engineering*, 50, pp. 72–84, 2013.  
<https://doi.org/10.1016/j.soildyn.2013.02.011>
- [16] Rizzitano S, Cascone E, Biondi G. "Coupling of topographic and stratigraphic effects on seismic response of slopes through 2D linear and equivalent linear analyses", *Soil Dynamics and Earthquake Engineering*, 67, pp. 66–84, 2014.  
<https://doi.org/10.1016/j.soildyn.2014.09.003>
- [17] Zhang, Y.-L., Ding, X.-M., Chen, Z.-X., Wu, Q., Wang, C.-L. "Seismic responses of slopes with different angles in coral sand", *Journal of Mountain Science*, 18(9), pp. 2475–2485, 2021.  
<https://doi.org/10.1007/s11629-020-6546-9>
- [18] Zhang, Z., Fleurisson, J.-A., Pellet, F. "The effects of slope topography on acceleration amplification and interaction between slope topography and seismic input motion", *Soil Dynamics and Earthquake Engineering*, 113, pp. 420–431, 2018.  
<https://doi.org/10.1016/j.soildyn.2018.06.019>
- [19] Assimaki, D., Kausel, E. "Modified topographic amplification factors for a single-faced slope due to kinematic soil-structure interaction", *Journal of Geotechnical and Geoenvironmental Engineering*, 133(11), pp. 1414–1431, 2007.  
[https://doi.org/10.1061/\(ASCE\)1090-0241\(2007\)133:11\(1414\)](https://doi.org/10.1061/(ASCE)1090-0241(2007)133:11(1414))
- [20] Pedersen, H., Le Brun, B., Hatzfeld, D., Campillo, M., Bard, P.-Y. "Ground-motion amplitude across ridges", *Bulletin of the Seismological Society of America*, 84(6), pp. 1786–1800, 1994.  
<https://doi.org/10.1785/BSSA0840061786>
- [21] Massa, M., Lovati, S., D'Alema, E., Ferretti, G., Bakavoli, M. "An experimental approach for estimating seismic amplification effects at the top of a ridge, and the implication for ground-motion predictions: The case of Narni, Central Italy", *Bulletin of the Seismological Society of America*, 100(6), pp. 3020–3034, 2010.  
<https://doi.org/10.1785/0120090382>
- [22] Geli, L., Bard, P.-Y., Jullien, B. "The effect of topography on earthquake ground motion: A review and new results", *Bulletin of the Seismological Society of America*, 78(1), pp. 42–63, 1988.  
<https://doi.org/10.1785/BSSA0780010042>
- [23] Buech, F., Davies, T. R., Pettinga, J. R. "The Little Red Hill Seismic Experimental Study: Topographic Effects on Ground Motion at a Bedrock-Dominated Mountain Edifice", *Bulletin of the Seismological Society of America*, 100(5A), pp. 2219–2229, 2010.  
<https://doi.org/10.1785/0120090345>
- [24] Wang, Y., Jin, G. "Seismic response characteristics of slopes in hilly districts based on experimental observations", *Bulletin of Engineering Geology and the Environment*, 81(10), 423, 2022.  
<https://doi.org/10.1007/s10064-022-02918-2>
- [25] Di Fiore, V. "Seismic site amplification induced by topographic irregularity: Results of a numerical analysis on 2D synthetic models", *Engineering Geology*, 114(3–4), pp. 109–115, 2010.  
<https://doi.org/10.1016/j.enggeo.2010.05.006>
- [26] Islamic Republic of Iran, Ministry of Housing and Urban Development, Building & Housing Research Center "Standard No. 2800 Iranian Code of Practice for Seismic Resistance Design of Buildings", 4th ed., Building & Housing Research Center, Tehran, Iran, 2015.
- [27] Yang, Y., Gong, W., Cheng, Y. P., Dai, G., Zou, Y., Liang, F. "Effect of soil-pile-structure interaction on seismic behavior of nuclear power station via shaking table tests", *Structures*, 33, pp. 2990–3001, 2021.  
<https://doi.org/10.1016/j.istruc.2021.06.051>
- [28] Ma, N., Wu, H., Ma, H., Wu, X., Wang, G. "Examining dynamic soil pressures and the effectiveness of different pile structures inside reinforced slopes using shaking table tests", *Soil Dynamics and Earthquake Engineering*, 116, pp. 293–303, 2019.  
<https://doi.org/10.1016/j.soildyn.2018.10.005>

- [29] Wang, C., Wang, H., Qin, W., Tian, H. "Experimental and numerical studies on the behavior and retaining mechanism of anchored stabilizing piles in landslides", *Bulletin of Engineering Geology and the Environment*, 80(10), pp. 7507–7524, 2021.  
<https://doi.org/10.1007/s10064-021-02391-3>
- [30] Bao, Y., Hu, H., Gan, G. "Seismic response analysis of slope reinforced by pile-anchor structures under near-fault pulse-like ground motions", *Soil Dynamics and Earthquake Engineering*, 164, 107576, 2023.  
<https://doi.org/10.1016/j.soildyn.2022.107576>
- [31] Chen, H., Jiang, G., Zhao, X., Zhu, D., Liu, Y., Tian, H. "Seismic Response Evaluation of High-Steep Slopes Supported by Anti-Slide Piles with Different Initial Damage Based on Shaking Table Test", *Materials*, 15(11), 3982, 2022.  
<https://doi.org/10.3390/ma15113982>
- [32] Hu, H., Huang, Y., Zhao, L., Xiong, M. "Shaking table tests on slope reinforced by anchored piles under random earthquake ground motions", *Acta Geotechnica*, 17(9), pp. 4113–4130, 2022.  
<https://doi.org/10.1007/s11440-022-01525-5>
- [33] Pai, L., Wu, H. "Shaking table test of comparison and optimization of seismic performance of slope reinforcement with multi-anchor piles", *Soil Dynamics and Earthquake Engineering*, 145, 106737, 2021.  
<https://doi.org/10.1016/j.soildyn.2021.106737>
- [34] Pai, L., Wu, H., Guan, W., Wei, H., Tang, L. "Shaking table test for seismic optimization of soil slope reinforced by new EPS pile under earthquake", *Soil Dynamics and Earthquake Engineering*, 154, 107140, 2022.  
<https://doi.org/10.1016/j.soildyn.2021.107140>
- [35] Tran, N. X., Gu, K.-Y., Yoo, M., Kim, S.-R. "Numerical evaluation of slope effect on soil–pile interaction in seismic analysis", *Applied Ocean Research*, 126, 103291, 2022.  
<https://doi.org/10.1016/j.apor.2022.103291>
- [36] Qu, L., Ding, X., Kouroussis, G., Zheng, C. "Dynamic interaction of soil and end-bearing piles in sloping ground: Numerical simulation and analytical solution", *Computers and Geotechnics*, 134, 103917, 2021.  
<https://doi.org/10.1016/j.compgeo.2020.103917>
- [37] Wood, D. M., Crewe, A., Taylor, C. "Shaking table testing of geotechnical models", *International Journal of Physical Modelling in Geotechnics*, 2(1), pp. 01–13, 2002.  
<https://doi.org/10.1680/ijpimg.2002.020101>
- [38] Bahadori, H., Ghalandarzadeh, A., Towhata, I. "Effect of non-plastic silt on the anisotropic behavior of sand", *Soils and Foundations*, 48(4), pp. 531–545, 2008.  
<https://doi.org/10.3208/sandf.48.531>
- [39] Ahmadi, M. M., Akbari Paydar, N. "Requirements for soil-specific correlation between shear wave velocity and liquefaction resistance of sands", *Soil Dynamics and Earthquake Engineering*, 57, pp. 152–163, 2014.  
<https://doi.org/10.1016/j.soildyn.2013.11.001>
- [40] Farahmand, K., Lashkari, A., Ghalandarzadeh, A. "Firoozkuh sand: Introduction of a benchmark for geomechanical studies", *Iranian Journal of Science and Technology, Transactions of Civil Engineering*, 40(2), pp. 133–148, 2016.  
<https://doi.org/10.1007/s40996-016-0009-0>
- [41] Komak Panah, A., Yazdi, M., Ghalandarzadeh, A. "Shaking table tests on soil retaining walls reinforced by polymeric strips", *Geotextiles and Geomembranes*, 43(2), pp. 148–161, 2015.  
<https://doi.org/10.1016/j.geotextmem.2015.01.001>
- [42] Yazdandoust, M. "Investigation on the seismic performance of steel-strip reinforced-soil retaining walls using shaking table test", *Soil Dynamics and Earthquake Engineering*, 97, pp. 216–232, 2017.  
<https://doi.org/10.1016/j.soildyn.2017.03.011>
- [43] Gohl, W. B. "Response of pile foundations to simulated earthquake loading: experimental and analytical results", *Doctoral dissertation*, University of British Columbia, 1991.  
<https://doi.org/10.14288/1.0050510>
- [44] Zhu, C., Cheng, H., Bao, Y., Chen, Z., Huang, Y. "Shaking table tests on the seismic response of slopes to near-fault ground motion", *Geomechanics and Engineering*, 29(2), pp. 133–143, 2022.  
<https://doi.org/10.12989/gae.2022.29.2.133>